공학석사학위논문

데이터 기반 모델 반전을 통한 6 자유도 유압식 굴착기의 모션 제어

Motion Control of 6-DOF Hydraulic Excavators via Data-Driven Model Inversion

2023 년 8 월

서울대학교 대학원

기계공학부

강 민 성

데이터 기반 모델 반전을 통한 6 자유도 유압식 굴착기의 모션 제어

Motion Control of 6-DOF Hydraulic Excavators via Data-Driven Model Inversion

지도교수 이 동 준

이 논문을 공학석사 학위논문으로 제출함

2023 년 4 월

서울대학교 대학원

기계공학부

강 민 성

강민성의 공학석사 학위논문을 인준함

2023 년 6 월

위 원 장 : 이 경 수 (인)

부위원장 : 이 동 준 (인)

위 원 : 이 윤 석 (인)

Abstract

Motion Control of 6-DOF Hydraulic Excavators via Data-Driven Model Inversion

Minsung Kang
Mechanical Engineering
The Graduate School
Seoul National University

In this study, we present the motion control of 6-degree-of-freedom (DOF) hydraulic excavators through data-driven model inversion. Due to their high degree of freedom, operating such 6-DOF excavators can be challenging, therefore there is a growing demand for autonomous control. However, their complex hydraulic characteristics pose a significant challenge to control. To address this issue, we adopt a modular approach to model the input delays, dead zones, and complex dynamics of the excavator based on a physics-inspired manner, and then train the model using real-world operation data. The resulting data-driven model is inverted to construct the controller. Our approach is validated through real-world experiments involving 6-DOF digging and grading tasks on a commercial hydraulic excavator, demonstrating accurate control performance (i.e., root-mean-square of horizontal and vertical path following errors under 4[cm]) even in the presence of soil interactions.

Keywords: Hydraulic excavator, Tilt-Rotator, Motion control, Data-driven, Soil interaction
Student Number: *2021-22988*

Contents

List of Figures

List of Tables

Abbreviations

DOF	**D**egree **O**f **F**reedom
MCV	**M**ain **C**ontrol **V**alve
PL	**P**iecewise **L**inear
IIR	**I**nfinite **I**mpulse **R**esponse
MLP	**M**ulti-**L**ayer **P**erceptron
RMSE	**R**oot **M**ean **S**quare **E**rror

Chapter 1

Introduction

1.1 Motivation and Background

Hydraulic excavators have been widely used in various industries, such as construction, mining, agriculture, and forestry, due to their high-power output. However, general excavators with standard buckets are typically limited to three degrees of freedom, consisting of the bucket, arm, and boom. Consequently, the reach and versatility of general excavators are limited, often requiring frequent movement of the excavator to reach inaccessible areas. For this reason, general excavators with standard buckets have problems with low productivity and efficiency. To address these challenges, third-party companies such as Engcon [1] or Steelwrist [2] have introduced new attachments, such as tilt-rotator, to enhance

FIGURE 1.1: Engcon tilt-rotator(left), Steelwrist tilt-rotator(right)

the functionality and flexibility of general excavators. A tilt-rotator attachment allows the operator to control the rotation and tilt angle of the excavator arm as shown in Figure 1.1, significantly improving the machine's range of motion and adaptability in various work environments. In recent years, tilt-rotator excavators have become increasingly popular due to their ability to handle more complex tasks, improve work efficiency, and reduce excavator movement on the job site.

Despite the advantages of tilt-rotators, it is difficult for unskilled users to use them due to the difficulty of simultaneously operating high degrees of freedom. Moreover, the aging workforce in construction sites and the scarcity of skilled workers have emphasized the need to develop automation technologies that simplify the operation of tilt-rotators for unskilled users. The development of such technologies not only aims to enhance usability but also improve safety in

high-risk construction environments. By addressing these challenges, automation technology can empower unskilled users to operate tilt-rotators more effectively while ensuring a safer working environment. However, while research on general excavators has been steadily progressing, the automatic control of tilt-rotator excavators has not been well studied.

1.2 Related Works

In general, hydraulic excavators are difficult to control precisely due to their nonlinearity, especially since they control the hydraulic fluid flow from the pump by manipulating the spool of the main control valve (MCV) (as shown in Figure 1.2), which has input delays and dead zone characteristics.

Several conventional model-based control methods [3–7] have been employed in the standard excavator. However, due to the high nonlinearity in hydraulics and the complexity of MCV, accurate mathematical modeling of the MCV becomes unfeasible, resulting in limited control accuracy due to the simplification of the excavator model. To overcome these difficulties, recent studies have focused on learning-based modeling approaches. Park [8, 9] employed recurrent neural network (RNN) techniques for controlling a general hydraulic excavator; however, the performance achieved was not highly satisfactory. Egli [10, 11] employed a reinforcement learning (RL) method for control, but the study had limitations

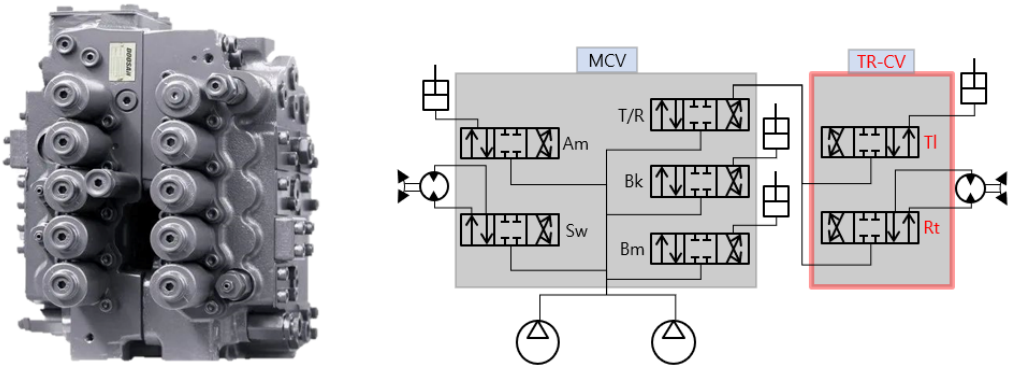

FIGURE 1.2: MCV(left), hydraulic circuit of MCV and TR control valve(right)

in terms of considering various tasks and soil interactions. Furthermore, the validation was limited to the slow-speed region, which is not representative of actual construction sites.

Some studies have been researched on model-based control methods for tilt-rotator excavators [12, 13]. Position and force control [12] has performed or velocity control [13] has been performed by simplifying the model, but these researches have solely been validated through only simulations without real-world experimental validation. While these studies have provided valuable insights, there remains a gap in research regarding practical control approaches for tilt-rotator excavators that consider the complexities of different tasks and soil interactions.

In the previous work [14], we successfully employed a physics-inspired data-driven model inversion approach to achieve precise control of a general excavator. This approach involved modeling the dead zone using a piecewise linear (PL) map,

input delays through an infinite impulse response (IIR) unit, and representing the excavator's complex dynamics and actuator coupling with MLP networks. By inversion of each of these modeled modules, we constructed an effective controller. The framework demonstrated its capability to achieve precise control in diverse work scenarios, accounting for soil interactions. In this paper, we extend the physics-inspired data-driven model inversion method used in our previous work to a 6-DOF tilt-rotator excavator.

1.3 Contribution

In this paper, we present the motion control for 6-degree-of-freedom (DOF) hydraulic excavators using data-driven model inversion. Our method focuses on a commercial 38-ton class hydraulic tilt-rotator excavator, equipped with various sensors such as IMUs, encoders, pressure sensors, and LiDAR. We extend the physics-inspired data-driven model inversion method to the tilt-rotator excavator, enabling precise and efficient motion control. To create the data-driven model, we gather real-world data from an autonomous excavator, ensuring the accuracy and relevance of our approach. To validate our method, we perform a comprehensive comparison between our data-driven model inversion and traditional trajectory tracking control methods. We evaluate the performance under various soil interaction environments, demonstrating the advantages of our approach. To further demonstrate the effectiveness of our approach, we conduct

real-world experiments involving 6-DOF digging and grading tasks on a commercial hydraulic excavator DX380LC. These experiments provide valuable insights into the practical applicability and robustness of our motion control strategy. Overall, our research offers a promising solution for enhancing the motion control capabilities of 6-DOF hydraulic excavators, paving the way for more efficient and accurate excavation operations in various scenarios.

The subsequent sections of this paper are organized as follows. Chapter 2 provides a comprehensive explanation of the system and base algorithm utilized in this study. In Chapter 3, we delve into the data-driven model inversion control method designed for autonomous excavators. Chapter 4 presents the detailed results obtained from experiments, covering both grading and digging tasks. Finally, in Chapter 5, we conclude this paper and outline future research.

Chapter 2

Preliminary

2.1 System Description

We employ the 38-ton HD HYUNDAI DEVELON DX380LC industrial hydraulic excavator, which is equipped with an Engcon tilt-rotator as shown in Figure 2.1., to validate the control performance. The excavator is attached with IMU sensors on the boom, arm, bucket guide link, tilt link, and cabin frame to measure their respective statuses. An encoder is also included to measure the swing and rotate angle and angular velocity. To gauge the pressure of the cylinder, hydraulic motor, and pump, pressure sensors are installed on the MCV. In addition, a LiDAR sensor is mounted on the boom to scan the terrain and gather point cloud data (PCD). Overall, the combined use of these sensors provides detailed

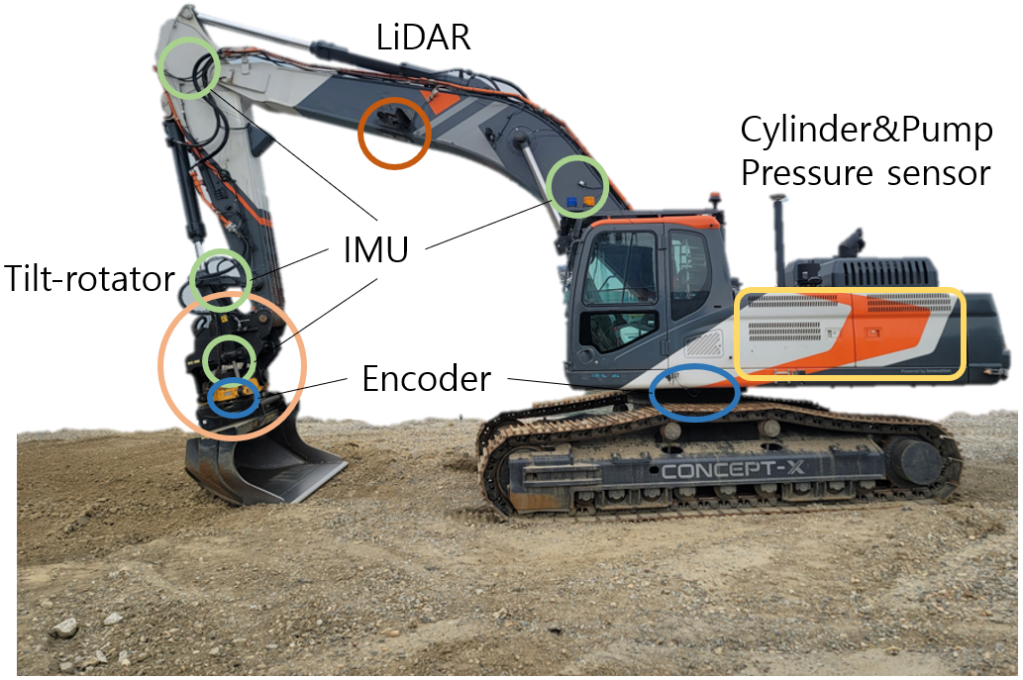

FIGURE 2.1: HD HYUNDAI DEVELON, 38-ton class hydraulic excavator equipped with tilt-rotator

and accurate data to analyze the excavator's end-effector path following control performances in real-world conditions.

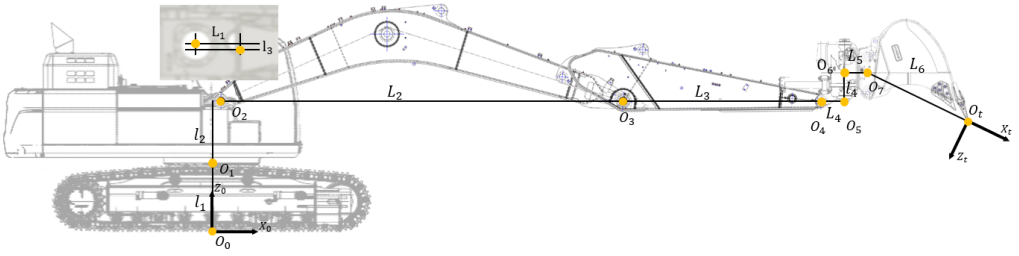

FIGURE 2.2: Tilt-Rotator excavator twists at the reference configuration

2.2 Tilt-Rotator Excavator Kinematic Analysis

For this study, we analyze the kinematic modeling of the 6-DOF rigid body manipulator of the tilt-rotator excavator. Instead of employing the conventional D-H (Denavit-Hartenberg) parameter method, we adopt the more efficient approach of analyzing the kinematics using screw theory. This method allows for streamlined analysis of the high degree of freedom manipulator, enabling a more effective representation of the tilt-rotator excavator kinematics.

In section 2.2.1, we will analyze the forward kinematics to calculate the bucket tip position and orientation from the joint angle value, and in section 2.2.2, we will analyze the inverse kinematics to calculate the joint angle value from the position and orientation of the bucket tip.

2.2.1 Forward Kinematics

We analyze the kinematics of the tilt-rotator excavator using the product of exponentials method. The unit vector in the direction of the twist axis for the revolute joint of the tilt-rotator excavator are

$$\omega_1 = \omega_5 = \begin{pmatrix} 0 \\ 0 \\ 1 \end{pmatrix}, \omega_2 = \omega_3 = \omega_4 = \begin{pmatrix} 0 \\ -1 \\ 0 \end{pmatrix}, \omega_6 = \begin{pmatrix} 1 \\ 0 \\ 0 \end{pmatrix} \tag{2.1}$$

The coordinate origins are ($L_{12} = L_1 + L_2$)

$$\begin{gathered} q_1 = \begin{pmatrix} 0 \\ 0 \\ l_1 \end{pmatrix}, q_2 = \begin{pmatrix} L_1 \\ -l_3 \\ l_{12} \end{pmatrix}, q_3 = \begin{pmatrix} L_{12} \\ -l_3 \\ l_{12} \end{pmatrix} \\ q_4 = \begin{pmatrix} L_{123} \\ -l_3 \\ l_{12} \end{pmatrix}, q_5 = \begin{pmatrix} L_{1234} \\ -l_3 \\ l_{12} \end{pmatrix}, q_6 = \begin{pmatrix} L_{1234} \\ -l_3 \\ l_{124} \end{pmatrix} \end{gathered} \tag{2.2}$$

Twists of the tilt-rotator excavator are

$$\xi_1 = \begin{pmatrix} 0 \\ 0 \\ 0 \\ 0 \\ 0 \\ 1 \end{pmatrix}, \xi_2 = \begin{pmatrix} l_{12} \\ 0 \\ -L_1 \\ 0 \\ -1 \\ 0 \end{pmatrix}, \xi_3 = \begin{pmatrix} l_{12} \\ 0 \\ -L_{12} \\ 0 \\ -1 \\ 0 \end{pmatrix}$$
$$\xi_4 = \begin{pmatrix} l_{12} \\ 0 \\ -L_{123} \\ 0 \\ -1 \\ 0 \end{pmatrix}, \xi_5 = \begin{pmatrix} -l_3 \\ -L_{1234} \\ 0 \\ 0 \\ 0 \\ 1 \end{pmatrix}, \xi_6 = \begin{pmatrix} 0 \\ l_{124} \\ l_3 \\ 1 \\ 0 \\ 0 \end{pmatrix} \tag{2.3}$$

The forward kinematics eqeuation of the tilt-rotator excavator is

$$T(\theta) = e^{\xi_1\theta_1} e^{\xi_2\theta_2} e^{\xi_3\theta_3} e^{\xi_4\theta_4} e^{\xi_5\theta_5} e^{\xi_6\theta_6} M(0) \tag{2.4}$$

where $M(0) \in SE(3)$ is the bucket tip position and orientation when the tilt-rotator excavator is in its zero position.

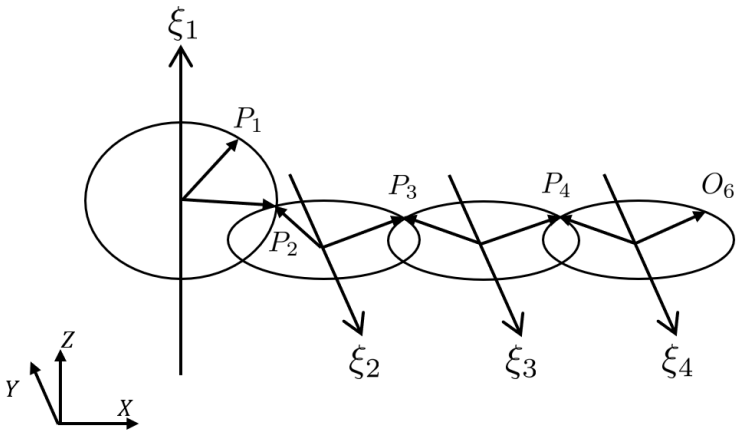

FIGURE 2.3: Screw motion of the swing, boom, arm, bucket joints

2.2.2 Inverse Kinematics

In general, inverse kinematics for high degree-of-freedom robots often pose challenges, as they can result in multiple solutions or even no solutions. To overcome these complexities, we leverage the unique structural characteristics of the tilt-rotator excavator to conduct an inverse kinematic analysis using analytical methods.

- Structural Property (non-spherical wrist as shown in Fig. 2.2)
  - ξ_5, ξ_6 are intersecting at a point (O_6) (can cancel θ_5, θ_6)
  - ξ_2, ξ_3, ξ_4 are parallel to each other

  $\rightarrow$ cut the 6R-chain into 4R- and a 2R-chain to solve inverse kinematics

⟨**Step-1. Calculate -** θ_1⟩

Right-multiplying Eq. 2.4 by $M(0)$.

$$T(\theta)M(0)^{-1} = e^{\xi_1\theta_1}e^{\xi_2\theta_2}e^{\xi_3\theta_3}e^{\xi_4\theta_4}e^{\xi_5\theta_5}e^{\xi_6\theta_6} \tag{2.5}$$

Since the twist motions of ξ_5, ξ_6 do not move the point O_6 as it is on both the axes of ξ_5, ξ_6, so we right-multiply by O_6 to omit both axes.

$$\begin{aligned} T(\theta)M(0)^{-1}O_6 &= e^{\xi_1\theta_1}(e^{\xi_2\theta_2}e^{\xi_3\theta_3}e^{\xi_4\theta_4})e^{\xi_5\theta_5}e^{\xi_6\theta_6}O_6 \\ P_1 &= e^{\xi_1\theta_1}(e^{\xi_2\theta_2}e^{\xi_3\theta_3}e^{\xi_4\theta_4})O_6 = (P_{x1}, P_{y1}, P_{z1})^T \end{aligned} \tag{2.6}$$

The equation 2.6 represents that ξ_2, ξ_3, ξ_4 all move O_6 on the (x, z)-plane (i.e., sagittal plane), while only the ξ_1-twist will produce the out plane motion of O_6 from the (x, z)-plane. (as shown in Fig. 2.3)

According to the screw motion, we can solve

$$\begin{cases} (P_2 - O_6) \cdot \omega_2 = 0 \\ (P_2 - r_1) \cdot \omega_1 = 0 \\ ||P_2 - r_1|| = ||P_1 - r_1|| \end{cases} \tag{2.7}$$

We can obtain point P_2 using equation 2.7

$$P_2 = (\sqrt{{P_{x1}}^2 + {P_{y1}}^2 - O_6(2)^2}, O_6(2), P_{z1})^T \tag{2.8}$$

Finally, we can obtain θ_1 by adopting the Paden-Kahan subproblem-1 [15].

$$P_1 = e^{\xi_1 \theta 1} \cdot P_2 \tag{2.9}$$

$\langle$**Step-2. Calculate -** θ_5**,** $\theta_6\rangle$

Left-multiplying Eq. 2.6 by $e^{-\xi\theta_1}$

$$\begin{aligned} e^{-\xi\theta_1} T(\theta) M(0)^{-1} &= e^{\xi_2\theta_2} e^{\xi_3\theta_3} e^{\xi_4\theta_4} e^{\xi_5\theta_5} e^{\xi_6\theta_6} \\ T_2(\theta) &= e^{\xi_2\theta_2} e^{\xi_3\theta_3} e^{\xi_4\theta_4} e^{\xi_5\theta_5} e^{\xi_6\theta_6} \end{aligned} \tag{2.10}$$

$$T_2(\theta) = \begin{bmatrix} R_{x1} & R_{y1} & R_{z1} & H_1 \\ R_{x2} & R_{y2} & R_{z2} & H_2 \\ R_{x3} & R_{y3} & R_{z3} & H_3 \\ 0 & 0 & 0 & 1 \end{bmatrix} \tag{2.11}$$

We use only orientation.

$$e^{\omega^{'}\theta_{234}} e^{\omega_5\theta_5} e^{\omega_6\theta_6} = \begin{bmatrix} R_{x1} & R_{y1} & R_{z1} \\ R_{x2} & R_{y2} & R_{z2} \\ R_{x3} & R_{y3} & R_{z3} \end{bmatrix}, (\omega_2 = \omega_3 = \omega_4 = \omega_{'}) \tag{2.12}$$

Then, we can obtain

$$\begin{aligned}\theta_5 &= \text{atan2}(R_{x2}, \sqrt{1 - R_{x2}^2}) \\ \theta_6 &= \text{atan2}(\frac{-R_{z2}}{\cos\theta_5}, \frac{R_{y2}}{\cos\theta_5}) \\ \theta_{234} &= \text{atan2}(\frac{R_{z1}}{\cos\theta_5}, \frac{R_{x1}}{\cos\theta_5})\end{aligned} \tag{2.13}$$

$\left\langle \textbf{Step-3. Calculate - } \theta_2, \theta_3, \theta_4 \right\rangle$

Right-multiplying Eq. 2.10 by $e^{-\xi_6\theta 6}$, $e^{-\xi_5\theta 5}$

$$\begin{aligned}T_2(\theta)e^{-\xi_6\theta_6}e^{-\xi_5\theta_5} &= e^{\xi_2\theta_2}e^{\xi_3\theta_3}e^{\xi_4\theta_4} \\ T_3(\theta) &= e^{\xi_2\theta_2}e^{\xi_3\theta_3}e^{\xi_4\theta_4}\end{aligned} \tag{2.14}$$

$$T_3(\theta) = \begin{bmatrix} r_{x1} & r_{y1} & r_{z1} & h_1 \\ r_{x2} & r_{y2} & r_{z2} & h_2 \\ r_{x3} & r_{y3} & r_{z3} & h_3 \\ 0 & 0 & 0 & 1 \end{bmatrix} \tag{2.15}$$

We use only position.

$$\begin{aligned}t_1 &= L_1 + L_2\cos\theta_2 + L_3\cos(\theta_{23}) - (L_{123}\cos(\theta_{234}) + l_{12}\sin(\theta_{234}) \\ t_3 &= l_{12} + L_2\sin\theta_2 + L_3\sin(\theta_{23}) - (L_{123}\sin(\theta_{234}) - l_{12}\cos(\theta_{234}) \\ t_4 &= L_2\cos\theta_2 + L_3\cos(\theta_{23}) \\ t_5 &= L_2\sin\theta_2 + L_3\sin(\theta_{23})\end{aligned} \tag{2.16}$$

Then, we can obtain

$$\begin{aligned} \theta_3 &= \text{atan2}(-\sqrt{(2L_2L_3)^2 - (t_4^2 + t_5^2 - L_2^2 - L_3^2)^2}, t_4^2 + t_5^2 - L_2^2 - L_3^2) \\ \theta_2 &= \text{atan2}(x_3, \sqrt{1 - x_3^2}) \\ \theta_4 &= \theta_{234} - (\theta_2 + \theta_3) \end{aligned} \tag{2.17}$$

where, $x_3 = \dfrac{(L_2 + L_3\cos\theta_3)t_5 - L_2\sin\theta_3 t_4}{(L_2 + L_3\cos\theta_3)^2 + (L_2\sin\theta_3)^2}$

2.3 Tilt-Rotator Excavator Dynamic Analysis

For this study, we analyze the dynamic modeling of the 6-DOF rigid body manipulator of the tilt-rotator excavator. The tilt-rotator excavator dynamic model is

$$M(\theta)\ddot{\theta} + C(\theta, \dot{\theta})\dot{\theta} + g(\theta) + \tau_f = \tau_u + J_{\text{tip}}^T \mathcal{F}_{\text{ext}} \tag{2.18}$$

where $\theta = [\theta_{swing}, \theta_{boom}, \theta_{arm}, \theta_{bucket}, \theta_{tilt}, \theta_{rotor}] \in \Re^6$ is the joint angle of the tilt-rotator excavator(as shown in Fig. 2.4), $M(\theta)$ is inertia matrix, $C(\theta, \dot{\theta})$ is the Coriolis and centripetal matrix, $g(\theta)$ is the gravity term, τ_f is the friction torques, τ_u is input torque, and $\mathcal{F}_{\text{ext}}$ is external wrenches.

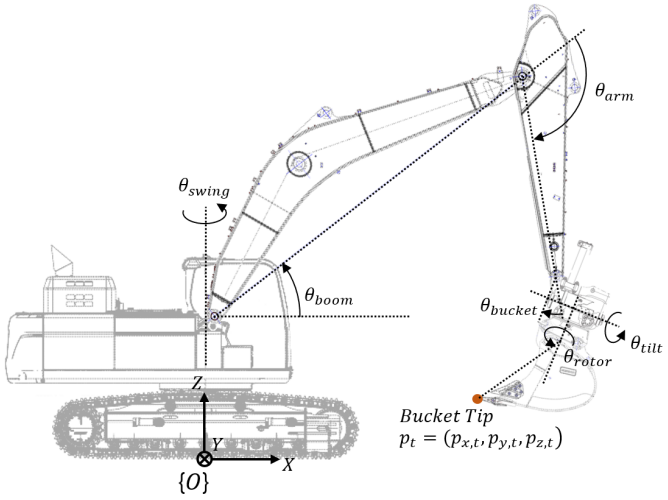

FIGURE 2.4: Joint configuration of the 6-DOF tilt-rotator excavator

2.4 External Wrench Estimation via Momentum Based Observer

Excavators operate in diverse soil interaction scenarios, where predicting external forces becomes challenging. To ensure precise control of the excavator, accounting for these external forces is imperative. However, measuring external forces directly by attaching a force/torque sensor on the bucket tip is not feasible. To overcome this limitation, our study adopts a momentum-based disturbance observer [16], [17], enabling real-time estimation of digging forces. By leveraging this method, we can calculate external forces while considering nonlinearities and coupling effects on the robot's inertia matrix. The equation is

$$
\begin{aligned}
\tau_{\text{ext}} &= K_0\left(p(t) - \int_0^t (\tau_u + \tau_f - \hat{\beta}(q,\dot{q}) + \tau_{\text{ext}})ds - p(0)\right) \\
p(t) &= M(q)\dot{q} \\
\beta(q,\dot{q}) &= -C^T(q,\dot{q})\dot{q} + g(q) \\
\mathcal{F}_{\text{ext}} &= J_{\text{tip}}^{-T}\tau_{ext}
\end{aligned}
\tag{2.19}
$$

where K_0 is the gain of the momentum based observer, θ and $\dot{\theta}$ are the joint angle and angular velocity can be gauged by IMU and encoder, τ_u can be calculated by cylinder and motor pressure sensors.

Chapter 3

Data-Driven Control

3.1 Control Architecture

In the previous work [14], we introduced the data-driven control architecture about standard excavator. This architecture is seamlessly applied to the tilt-rotator excavator control, as shown in Fig 3.1. Here's a step-by-step explanation of the control process:

- Trajectory Planner: The trajectory planner generates trajectories for various tasks that the excavator needs to perform, such as digging and grading. It calculates the desired joint angles and angular velocities for these trajectories.

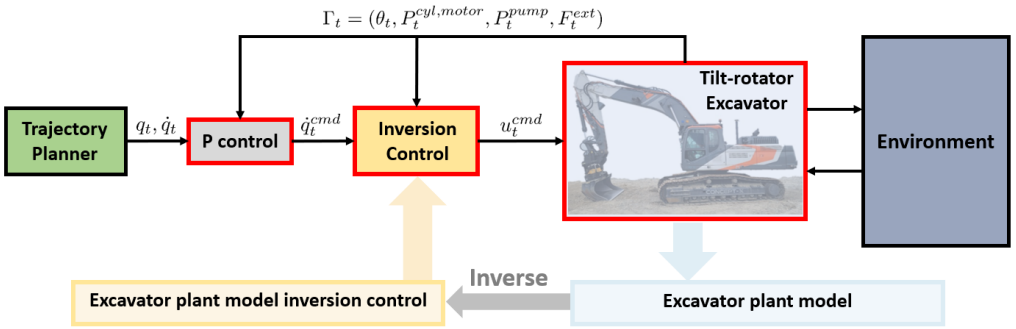

FIGURE 3.1: Control architecture of the data-driven model inversion

- P Controller: The generated joint desired angles undergo P controller processing to enhance controller robustness. The P controller generates joint angular velocity commands based on the desired angles and angular velocities, ensuring robust control during operation.

- Inversion Controller: The model inversion controller is responsible for autonomous operation. It generates a joystick signal using the joint angular velocity commands obtained from the P controller. This enables the excavator to execute tasks autonomously.

The model inversion controller is developed by inversion the excavator plant model, which is created based on real excavator work data. This approach ensures that the excavator's control system effectively adapts to real-world conditions and facilitates accurate and reliable autonomous operation.

3.2 Designing Data-Driven Model Inversion

The tilt-rotator excavator plant model is presented, comprising three modules, as illustrated in Fig. 3.2. The plant model consists of a pre-delay map, that is piecewise linear (PL) map, which considers the dead zone of excavator hydraulics, a delaying system, that is an infinite impulse response (IIR) unit, which considers the input delay, and a post-delay map, that is multi-layer perceptron (MLP), which considers the coupled dynamics of complex main control valve(MCV). The equations for each module are provided below.

$$\begin{aligned} \eta_{f,t} &= f_{\Gamma_t}(u_t) \\ \mathcal{Z}\{\eta_{h,t}\} &= P(z)\mathcal{Z}\{\eta_{f,t}\} \\ \hat{\omega_t} &= h_{\Gamma_t} u_t \end{aligned} \tag{3.1}$$

where $P(z)$ is the delaying system (IIR unit), and $\mathcal{Z}$ is z-transform. The joystick input is expressed in $u_t \in \mathbb{R}^6$, the joint angular velocity is expressed in $\omega_t \in \mathbb{R}^6$, t is the time step, and the tilt-rotator excavator state is expressed in

$$\Gamma_t = (\theta_t, P_t^{cyl}, P_t^{motor}, P_t^{pump}, F_t^{ext}) \in \mathbb{R}^{19} \tag{3.2}$$

where $\theta_t = (\theta_t^{swing}, \theta_t^{boom}, \theta_t^{arm}, \theta_t^{bucket}, \theta_t^{tilt}, \theta_t^{rotor}) \in \mathbb{R}^6$ in the joint angle, $P_t^{cyl} \in \mathbb{R}^6$ is the pressure of both side cylinder, $P_t^{motor} \in \mathbb{R}^2$ is the pressure of left and right swing motor, $P_t^{pump} \in \mathbb{R}^2$ is the pressure of master and slave pumps, and $F_t^{ext} \in \mathbb{R}^3$ is the external forces acting on the bucket tip.

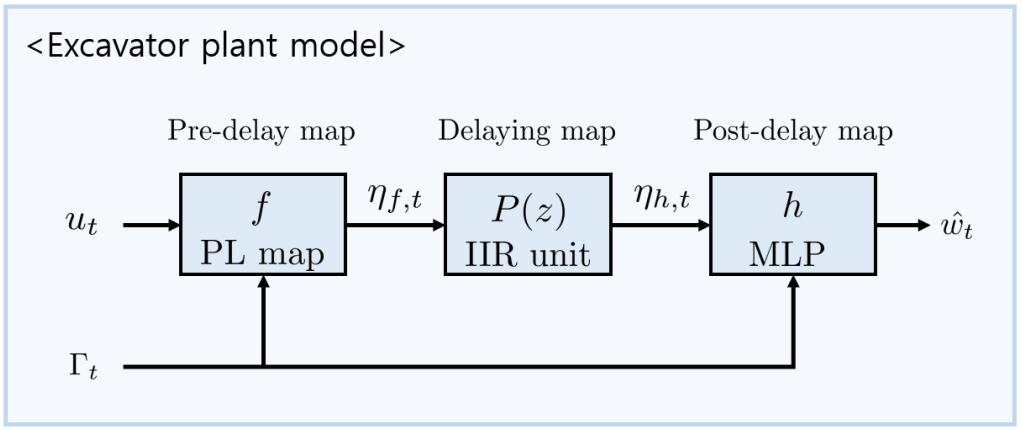

FIGURE 3.2: Tilt-rotator excavator plant model

The plant model inversion control is constructed by inverting the plant model, as shown in Fig. 3.3. The plant model inversion control consists of a pre-control map, which is the inversion of a post-delay map, a delaying-tracking, which is the inversion of a delaying system, and a post-control map, which is the inversion of a pre-delay map. The equations for each module are provided below.

$$\begin{aligned} \zeta_{h,t} &= g_{h,\Gamma_t}(\omega_t^{cmd}) \\ \mathcal{Z}\{\zeta_{f,t}\} &= C_P(z)\mathcal{Z}\{\zeta_{h,t}\} \\ u_t &= g_{f,\Gamma_t}\zeta_{f,t} \end{aligned} \tag{3.3}$$

where $C_P(z)$ is the delay-tracking system, it is calculated from the final value theorem.

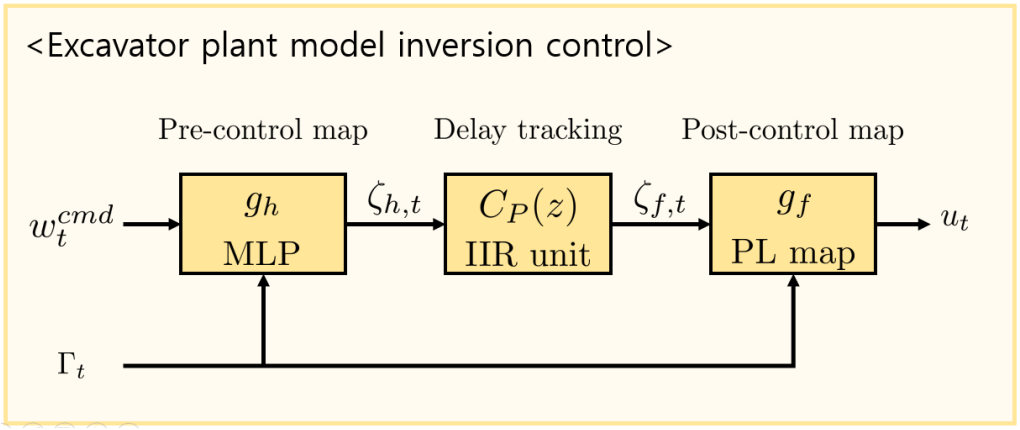

FIGURE 3.3: Tilt-rotator excavator model inversion control

3.3 Learning Data-Driven Model Inversion

The data-driven model inversion construction involves two essential steps, as illustrated in Fig. 3.4. In the first step, we focus on learning the tilt-rotator excavator plant model, which encompasses the pre-delay map, delaying map, and post-delay map. The subsequent step involves obtaining the pre-control map through inversion learning of the post-delay map.

To facilitate the learning process, we collect sensor data from the DX380LC excavator, equipped with a tilt-rotator, specifically focusing on digging and grading tasks involving all 6-DOF as shown in Fig. 3.5. The data acquisition is executed through automated operations, while the reference path for autonomous operation is derived from scaling and transforming the nominal trajectory from human expert patterns [18].

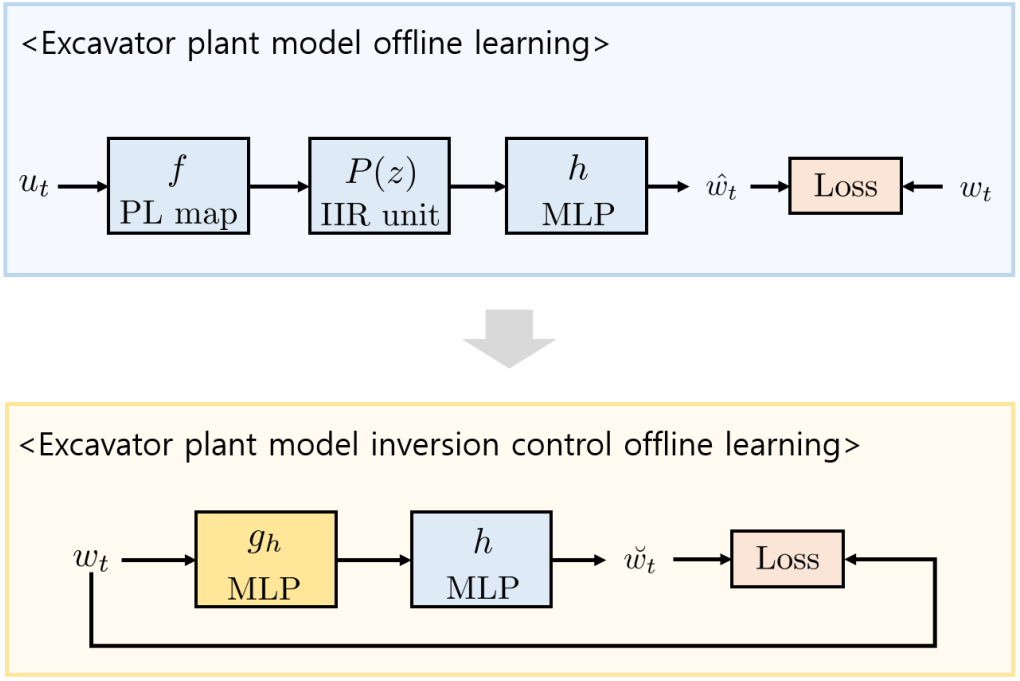

FIGURE 3.4: Model and inversion control learning schema

Our training dataset comprises 2 million time steps collected at a 100 [Hz], equivalent to approximately 5.5 hours of operational data. For training, we utilize a PC with an Intel(R) Xeon(R) Gold 6234 CPU (@ 3.30 GHz), 64.0GB of RAM, and an NVIDIA Quadro RTX 8000. The training process, until convergence, typically takes around 1.5 hours, ensuring the efficiency and effectiveness of the model inversion construction.

The first step involves learning the plant model of the tilt-rotator excavator using a supervised learning approach as shown in the top of Fig. 3.4. To achieve this,

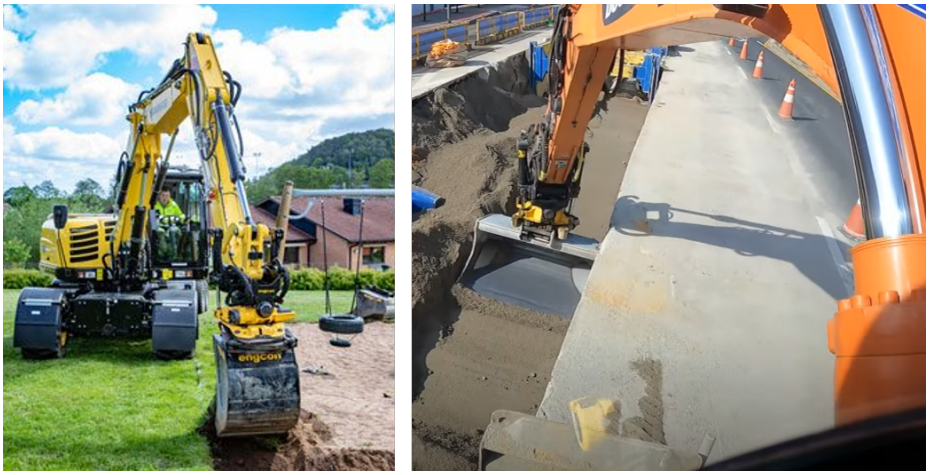

FIGURE 3.5: Tilt-rotator digging and grading tasks

we utilized the neural network modules (PL map, IIR unit, MLP) that were previously employed in our previous study for training purposes. The second step involves learning the pre-control map of the model inversion control using a supervised learning approach. We use a distal learning approach [19]. Fig. 3.6 and Fig. 3.7 show the trained PL map and characteristics of the delaying system.

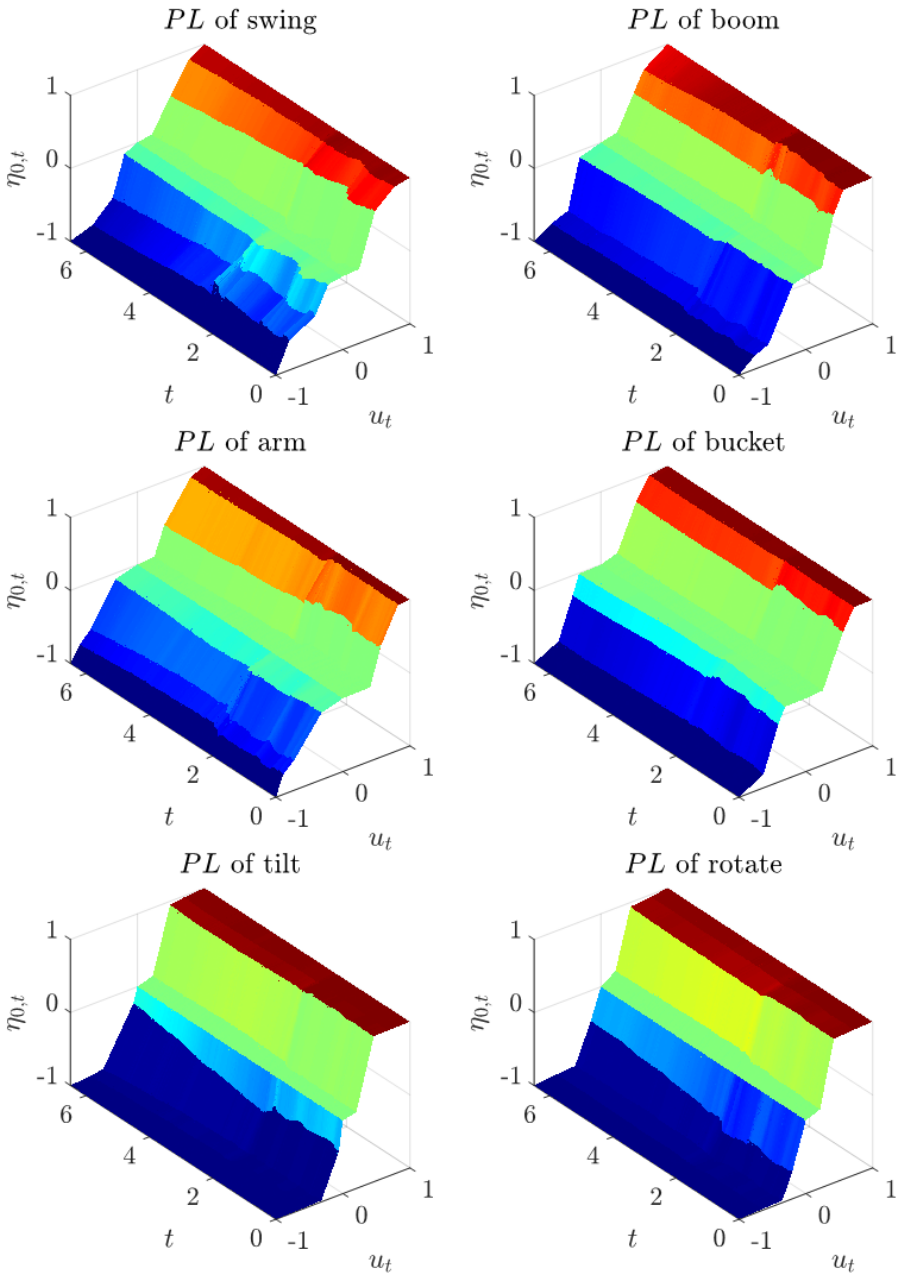

FIGURE 3.6: Pre-delay maps of the tilt-rotator excavator(PL map)

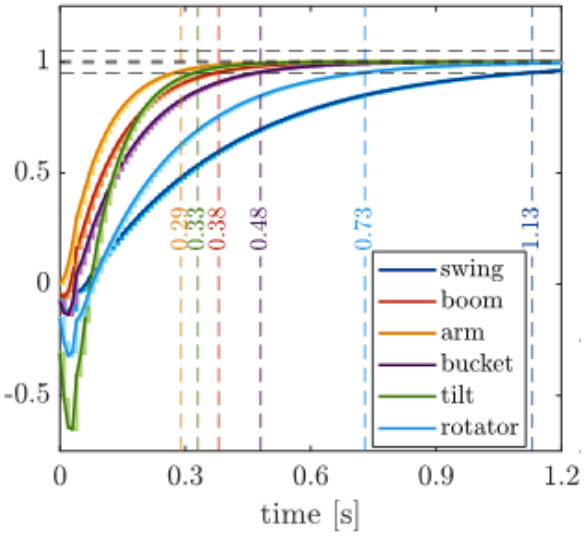

FIGURE 3.7: Delaying system of the tilt-rotator excavator(IIR unit)

Chapter 4

Experiment Results

4.1 Experiment Set Up

To evaluate the control performance of our approach, we conduct experiments using a commercially available 38-ton class tilt-rotator excavator, the HD HYUNDAI DEVELON (as shown in Figure 4.1), in digging and grading tasks. For the model inversion input, we select a proportional gain value of $K_p = 1.0I_6$. Based on the findings from the previous work, we determine that incorporating integral feedback was not necessary as the error remained small with P control alone, thus ensuring sufficient control performance.

We utilize the calculated position of the bucket tip p_t=($p_{x,t}$,$p_{y,t}$,$p_{z,t}$) (as shown in Figure 2.4) to evaluate the control performance. The vertical error, consisting of

FIGURE 4.1: Experiment environment using tilt-rotator excavator

the $p_{x,t}$ and $p_{z,t}$ positions, and the horizontal error, consisting of the $p_{x,t}$ and $p_{z,t}$ positions, are defined for evaluation purposes. To establish a basis for comparison, we contrast our control approach with the manufacturer's PI control system. By comparing our approach to the manufacturer's PI control, we can effectively evaluate the performance and effectiveness of our method.

4.2 Grading Result

Grading is leveling or shaping the ground surface to achieve a desired slope or contour (as shown in Figure 4.2). The manufacturer's PI control system results showed a path following RMSE of 7.85 [cm] in the vertical direction and 7.21

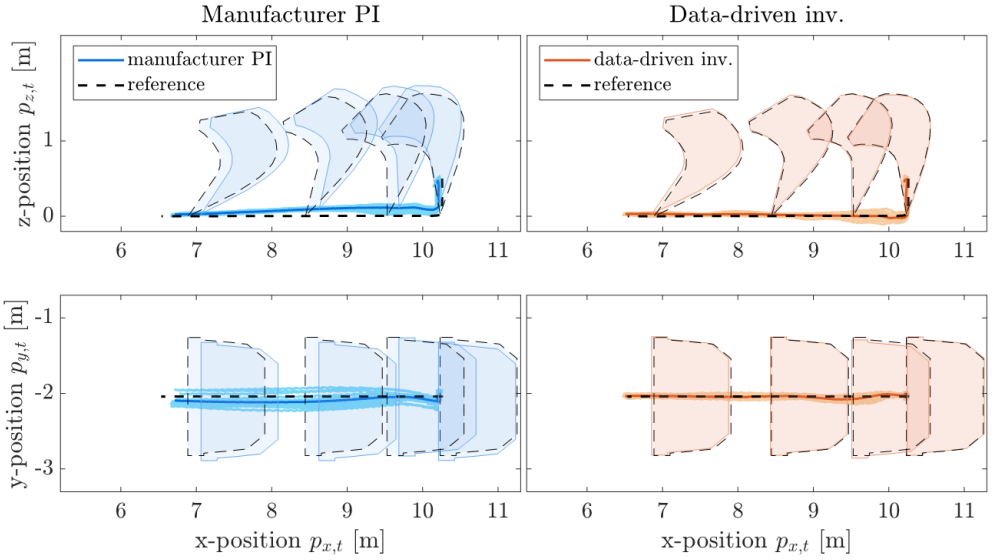

FIGURE 4.2: Bucket tip position during the grading operation

[cm] in the horizontal direction. Additionally, the trajectory RMSE is found to be 16.99 [cm] vertically and 15.46 [cm] horizontally. In contrast, our system demonstrates superior performance, outperforming the manufacturer-provided PI control. Specifically, our framework achieves a significant reduction in path following RMSE, with vertical and horizontal values of 3.58 [cm] and 2.94 [cm], respectively. Moreover, the trajectory RMSE is significantly improved to 4.88 [cm] vertically and 4.35 [cm] horizontally (see Table 4.1). As more data is added, we observe a progressive improvement in the control performance (as shown in Fig. 4.4).

		Manufacture PI	Data-driven inv.
Trj. Tracking	Vert.	16.99	**4.88**
RMSE [cm]	Hori.	15.46	**4.35**
Path Following	Vert.	7.85	**3.58**
RMSE [cm]	Hori.	7.21	**2.94**

Table 4.1: Control accuracy of the bucket tip positions during the grading tasks

4.3 Digging Result

Digging, a fundamental process involving the removal of materials such as soil and rocks from the ground, is performed extensively to reach the desired ground level in our experiments (as shown in Figure 4.3). The manufacturer's PI control system results showed a path following RMSE of 5.06 [cm] in the vertical direction and 5.03 [cm] in the horizontal direction. Additionally, the trajectory RMSE is found to be 17.65 [cm] vertically and 17.95 [cm] horizontally. In contrast, our system demonstrates superior performance, outperforming the manufacturer-provided PI control. Specifically, our framework achieves a significant reduction in path following RMSE, with vertical and horizontal values of 3.45 [cm] and 2.97 [cm], respectively. Moreover, the trajectory RMSE is significantly improved to 8.11 [cm] vertically and 8.06 [cm] horizontally (see Table 4.2). As more data

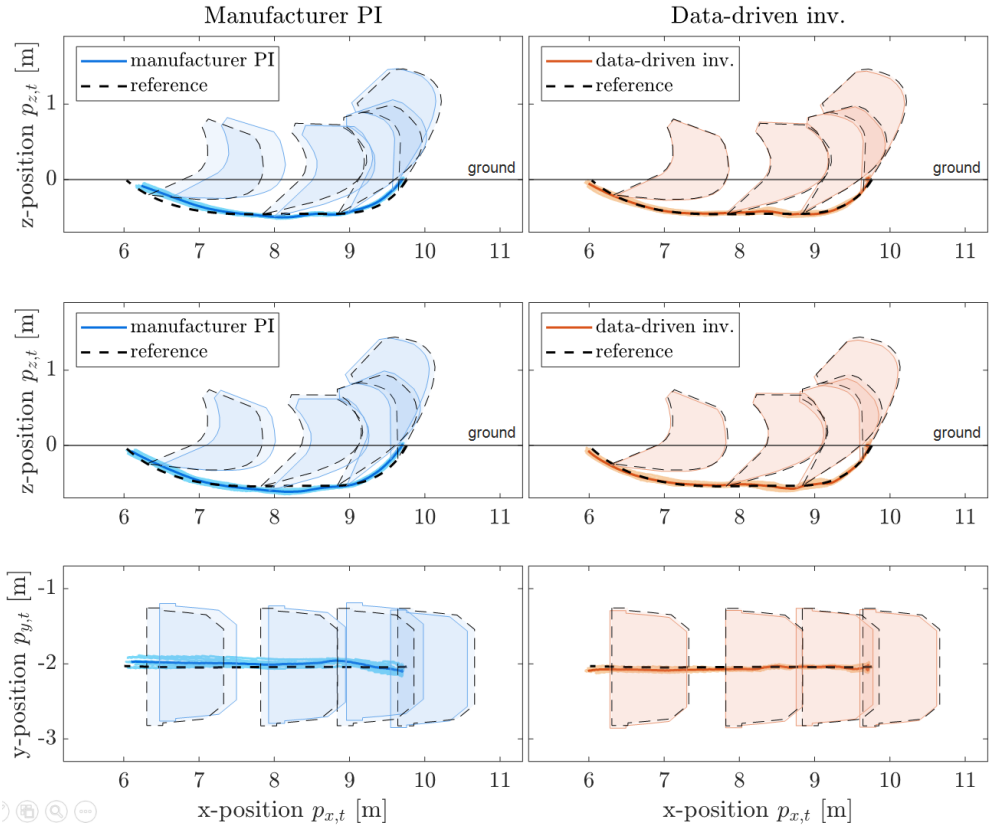

FIGURE 4.3: Bucket tip position during the digging operation

is added, we observe a progressive improvement in the control performance (as shown in Fig. 4.4).

		Manufacture PI	Data-driven inv.
Trj. Tracking	Vert.	17.65	**8.11**
RMSE [cm]	Hori.	17.95	**8.06**
Path Following	Vert.	5.06	**3.45**
RMSE [cm]	Hori.	5.03	**2.97**

Table 4.2: Control accuracy of the bucket tip positions during the digging tasks

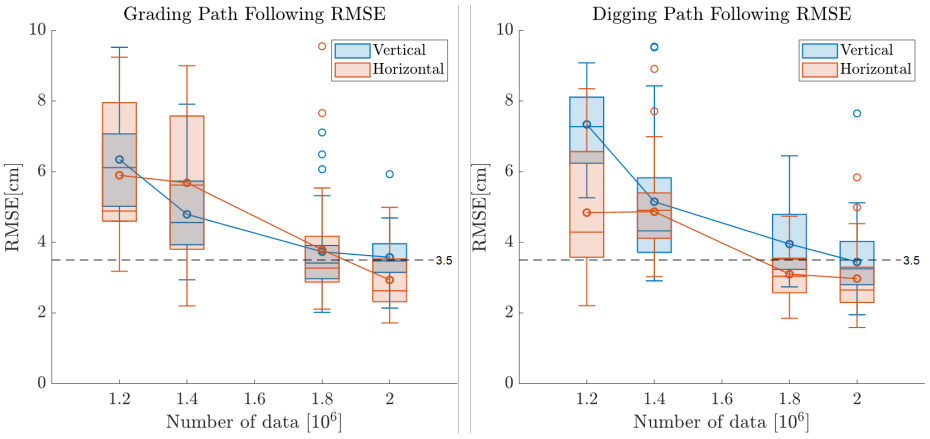

FIGURE 4.4: Bucket tip accuracy about grading and digging tasks by adding the number of data

Chapter 5

Conclusion and Future Work

5.1 Conclusion

In this paper, we successfully construct an autonomous 6-DOF tilt-rotator excavator that applied the data-driven model inversion method. First, we analyzed the kinematics and dynamics of a 6-DOF tilt-rotator excavator. Then, we applied an MBO-based external force estimator to calculate the external force acting on the bucket tip in real-time. For autonomous excavator control, we generate a tilt-rotator excavator model based on real-world data and construct a controller by inversion of the generated model.

To validate our study, we conduct an experiment using an actual excavator and compare its performance with the traditional PI control provided by the manufacturer. The results of the experiment clearly demonstrate that our control method outperforms the manufacturer's PI control in terms of performance and precision (i.e., root-mean-square of horizontal and vertical path following errors under 4[cm]) even in the presence of soil interactions. These findings highlight the potential of the data-driven model inversion approach in enhancing the control capabilities of tilt-rotator excavators, leading to more precise and effective operation in various tasks and work environments.

Overall, our research represents an important step forward in the automation of 6-DOF tilt-rotator excavators. By leveraging data-driven model inversion, we pave the way for more precise and effective excavation operations across various tasks and work environments.

FIGURE 5.1: Various attachments for the excavator

5.2 Future Work

In future works, we aim to extend the application of our framework to encompass a wider range of attachments. While recent research focuses on gripper [20–22] or harvester [23, 24] attachments, other essential attachments, such as pallet forks,

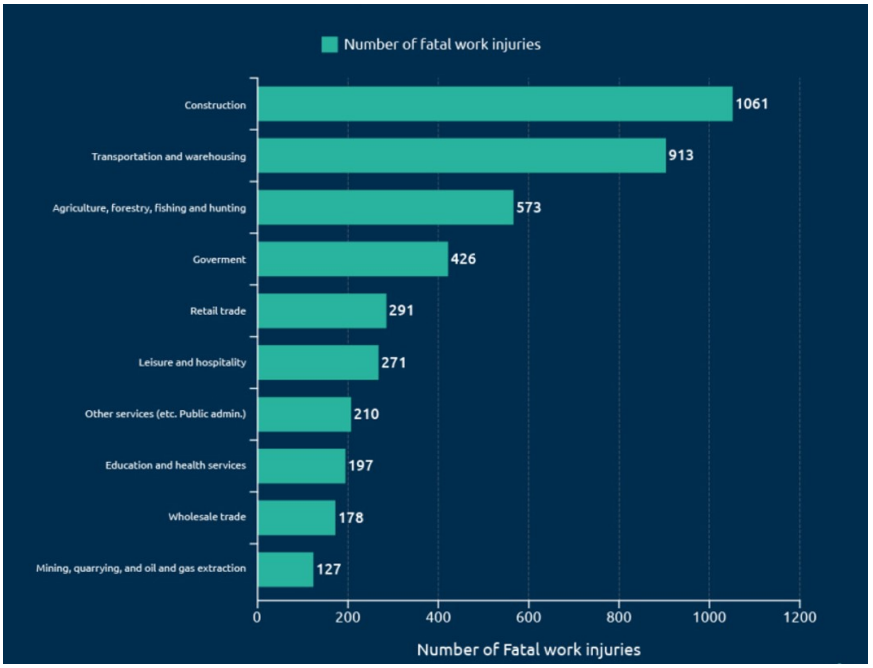

FIGURE 5.2: Number of fatal work injuries by industry sector

rollers, ripper, and compactors (as shown in Fig. 5.1), have received less attention. By encompassing these attachments in our framework, we aim to achieve precise control over various tasks and operational scenarios, further enhancing the versatility and applicability of our approach.

We also acknowledge the significance of addressing the aging characteristics of excavators and their implications on dynamic behavior. To tackle this challenge, we plan to develop a robust control framework capable of effectively adapting and responding to such variations. This enhancement will bolster the system's resilience, ensuring consistent and precise performance over extended periods.

Safety remains a paramount concern at construction sites, particularly considering the significant force exerted by excavators, resulting in heightened risks and an elevated probability of fatal accidents compared to other industries [25] as shown in Fig. 5.2. In response, we aim to conduct research from a safety perspective, focusing on preventing accidents during excavator autonomous work. Specifically, our objective is to implement real-time path regeneration to avert tipping-over or slipping incidents, proactively mitigating potential safety hazards.

By addressing these future works, we aspire to push the boundaries of our research, improving not only the operational capabilities but also the safety standards of excavator automation, and making a meaningful impact in the industry.

Bibliography

[1] Engcon - official website. https://engcon.com. Accessed: 2023-05-03.

[2] Steelwrist - official website. https://steelwrist.com. Accessed: 2023-05-03.

[3] Kwangmin Kim, Minji Kim, Dongmok Kim, and Dongjun Lee. Modeling and velocity-field control of autonomous excavator with main control valve. *Automatica*, 104:67–81, 2019.

[4] Shahram Tafazoli, Septimiu E Salcudean, Keyvan Hashtrudi-Zaad, and Peter D Lawrence. Impedance control of a teleoperated excavator. *IEEE Transactions on Control Systems Technology*, 10(3):355–367, 2002.

[5] Quang Ha, Miguel Santos, Quang Nguyen, David Rye, and Hugh Durrant-Whyte. Robotic excavation in construction automation. *IEEE Robotics & Automation Magazine*, 9(1):20–28, 2002.

[6] Pyung Hun Chang and Soo-Jin Lee. A straight-line motion tracking control of hydraulic excavator system. *Mechatronics*, 12(1):119–138, 2002.

[7] Jian Wang, Hao Zhang, Peng Hao, and Hua Deng. Observer-based approximate affine nonlinear model predictive controller for hydraulic robotic excavators with constraints. *Processes*, 11(7):1918, 2023.

[8] Jaemann Park, Dongsoo Cho, Seunghyun Kim, Young Bum Kim, Pan Young Kim, and H Jin Kim. Utilizing online learning based on echo-state networks for the control of a hydraulic excavator. *Mechatronics*, 24(8):986–1000, 2014.

[9] Jaemann Park, Bongju Lee, Seonhyeok Kang, Pan Young Kim, and H Jin Kim. Online learning control of hydraulic excavators based on echo-state networks. *IEEE Transactions on Automation Science and Engineering*, 14 (1):249–259, 2016.

[10] Pascal Egli and Marco Hutter. Towards rl-based hydraulic excavator automation. In *2020 IEEE/RSJ International Conference on Intelligent Robots and Systems (IROS)*, pages 2692–2697. IEEE, 2020.

[11] Pascal Egli and Marco Hutter. A general approach for the automation of hydraulic excavator arms using reinforcement learning. *IEEE Robotics and Automation Letters*, 7(2):5679–5686, 2022.

[12] Sami Päkkilä. Modeling and simulation of a six degrees of freedom excavator. Master's thesis, 2017.

[13] Timothy Fisher. *Simplified Vector-Directed Control of a Tiltrotator Equipped Excavator*. PhD thesis, The University of Alabama at Birmingham, 2019.

[14] Minhyeong Lee, Hyelim Choi, ChangU Kim, Jihyun Moon, Dongmok Kim, and Dongjun Lee. Precision motion control of robotized industrial hydraulic excavators via data-driven model inversion. *IEEE Robotics and Automation Letters*, 7(2):1912–1919, 2022.

[15] Richard M Murray, Zexiang Li, S Shankar Sastry, and S Shankara Sastry. *A mathematical introduction to robotic manipulation*. CRC press, 1994.

[16] Sami Haddadin, Alessandro De Luca, and Alin Albu-Schäffer. Robot collisions: A survey on detection, isolation, and identification. *IEEE Transactions on Robotics*, 33(6):1292–1312, 2017.

[17] Juhoon Back and Wonseok Ha. Robust tracking of robot manipulators via momentum-based disturbance observer and passivity-based controller. *International Journal of Control, Automation and Systems*, 17:976–985, 2019.

[18] Bukun Son, ChangU Kim, Changmuk Kim, and Dongjun Lee. Expert-emulating excavation trajectory planning for autonomous robotic industrial excavator. In *2020 IEEE/RSJ international conference on intelligent robots and systems (IROS)*, pages 2656–2662. IEEE, 2020.

[19] Michael I Jordan and David E Rumelhart. Forward models: Supervised learning with a distal teacher. In *Backpropagation*, pages 189–236. Psychology Press, 2013.

[20] Ryan Luke Johns, Martin Wermelinger, Ruben Mascaro, Dominic Jud, Fabio Gramazio, Matthias Kohler, Margarita Chli, and Marco Hutter. Autonomous dry stone: On-site planning and assembly of stone walls with a robotic excavator. *Construction Robotics*, 4(3-4):127–140, 2020.

[21] Ruben Mascaro, Martin Wermelinger, Marco Hutter, and Margarita Chli. Towards automating construction tasks: Large-scale object mapping, segmentation, and manipulation. *Journal of Field Robotics*, 38(5):684–699, 2021.

[22] Martin Wermelinger, Ryan Johns, Fabio Gramazio, Matthias Kohler, and Marco Hutter. Grasping and object reorientation for autonomous construction of stone structures. *IEEE Robotics and Automation Letters*, 6(3):5105–5112, 2021.

[23] Edo Jelavic, Dominic Jud, Pascal Egli, and Marco Hutter. Towards autonomous robotic precision harvesting: Mapping, localization, planning and control for a legged tree harvester. *arXiv preprint arXiv:2104.10110*, 2021.

[24] Edo Jelavic, Tun Kapgen, Simon Kerscher, Dominic Jud, and Marco Hutter. Harveri: A small (semi-) autonomous precision tree harvester. In *Innovation in Forestry Robotics: Research and Industry Adoption, ICRA 2022 IFRRIA Workshop*. ETH Zurich, Institute of Robotics and Intelligent Systems, 2022.

[25] U.S bureau of labor statistics. https://www.woodworkingnetwork.com/best-practices-guide/plant-production-software/

fatal-construction-accidents-rise-need-know. Accessed: 2023-05-03.

요약

본 논문에서는 데이터 기반 모델 반전을 통해 6자유도(DOF) 유압 굴착기의 자율 작업을 위한 모션 제어를 제시한다. 틸트로테이터가 장착된 6자유도 굴착기는 높은 자유도로 인해 작동이 까다로워 자율 제어에 대한 수요가 증가하고 있다. 그러나 복잡한 유압 특성으로 인해 제어에 상당한 어려움이 있다. 이러한 문제를 해결하기 위해 실제 굴착기 구조를 기반으로 모듈러 방식으로 굴착기의 입력 지연, 데드존, 복잡한 동역학을 모델링한 후에 실제 동작 데이터를 사용하여 모델을 학습하였다. 이렇게 만들어진 데이터 기반 모델을 반전시켜 컨트롤러를 구성하였다. 이러한 접근 방식은 상용 유압 굴착기에서 6-DOF 굴착 및 그레이딩 작업을 포함한 실제 실험을 통해 검증되었으며, 토양 상호작용이 있는 상황에서도 정확한 제어 성능(즉, 수평 및 수직 경로 추종 오차가 4[cm] 미만)을 입증하였다.

주요어: Hydraulic excavator, Tilt-Rotator, Motion control, Data-driven, Soil interaction

학번: *2021-22988*